*Geophys. J. Int.* (2006) **167,** 906–916 doi: 10.1111/j.1365-246X.2006.03085.x

# Three-dimensional lithospheric deformation and gravity anomalies associated with oblique continental collision in South Island, New Zealand

Martin Scherwath,[1] Tim Stern,[2] Fred Davey[3] and Rob Davies[4]

[1]*Leibniz Institut für Meereswissenschaften, IFM-GEOMAR, Kiel, Germany. E-mail: mscherwath@ifm-geomar.de*
[2]*School of Earth Sciences, Victoria University of Wellington, New Zealand*
[3]*Institute of Geological and Nuclear Sciences, Lower Hutt, New Zealand*
[4]*Department of Geography, University of Wales, Swansea, UK*

Accepted 2006 June 7. Received 2006 April 14; in original form 2005 March 31

## SUMMARY

Isostatic considerations exhibit differences between the northern, central and southern parts of the Pacific–Australian plate collision in South Island, New Zealand. In the northern part mean elevations are moderate and the gravity low is small; the central part contains the highest elevations, and gravity and elevations correspond to each other relatively well; and in the southern part the gravity low is strongest whereas the mean elevations are moderate again. These differences indicate changes in the character of the isostatic compensation and are explained by increased thickening and widening of the crustal root from north to south, and also by the long wavelength gravity response to a mantle density anomaly that increases towards the south. A simple 3-D gravity model is derived that includes the detailed crustal structures from the South Island GeopHysical Transect (SIGHT) experiment as well as a high-density anomaly in the mantle inferred from teleseismic data. The model indicates that cold and, therefore, dense upper mantle material penetrates the asthenosphere to a greater extent in the south, similar to the behaviour of an apparently highly ductile lower crust. As plate reconstruction suggests more lithospheric shortening in the north, our model corresponds to lithospheric material escaping laterally to the south, almost perpendicular to the compression caused by lithospheric shortening of the mantle. Therefore, in addition to the prevailing mantle shear in New Zealand, there may also be a component of extrusional mantle creep beneath the Southern Alps orogen, which could have caused some of the observed large seismic anisotropy in this region. We may have also found evidence for submerged Eocene–Miocene oceanic lithosphere beneath the southeastern part of South Island that has been unaccounted for after plate reconstruction.

**Key words:** continental collision, creep, gravity anomalies, isostasy, lithospheric deformation, South Island.



## 1 INTRODUCTION

When tectonic plates collide, the lithosphere becomes compressed, and this has to be accommodated by either subduction, thickening and/or lateral escape of lithospheric material. Collision in continental regimes causes mountain building in the crust; however, the lithospheric mantle can still be subject to either subduction or thickening (Houseman *et al.* 1981; Sutherland *et al.* 2000; Pysklywec *et al.* 2002). Lithospheric thickening differs fundamentally from intracontinental subduction as a means of shortening mantle lithosphere. While subduction is inherently asymmetric with strain concentrated on a single interface (the subduction thrust), during lithospheric thickening the strain is distributed, and this process has a symmetry that links both crustal thickening and the subjacent thickening mantle lithosphere. Upper, lithospheric mantle material placed in the asthenospheric mantle forms a so-called 'blob' through Rayleigh–Taylor instability (Houseman & Molnar 1997), and produces downwelling, since upper mantle material within the asthenosphere is relatively colder and, therefore, denser.

Continental collision is often also accompanied by lateral extrusion in the form of mantle creep as inferred from seismic anisotropy in the mantle (Vauchez & Nicholas 1991; Meissner *et al.* 2002). Usually in younger and hotter orogens the lower crust is relatively ductile and cannot sustain all of the induced weight from the collision, which causes the lower crust to delaminate and, part of it, to 'escape' sideways (e.g. Tapponnier *et al.* 1982; Bird 1991). This process consequently influences the entire lithospheric deformation and induces the mantle creep that leads to the observed seismic

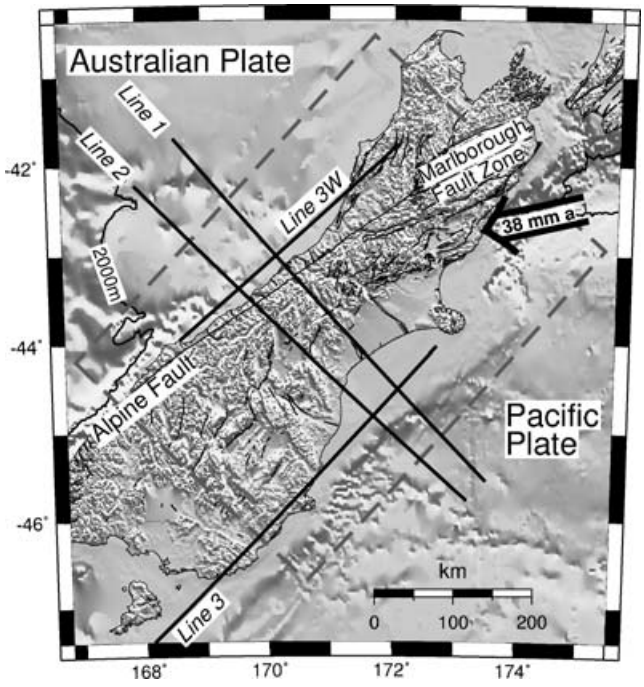


**Figure 1.** Oblique compression across the plate boundary in South Island, New Zealand. Thick black lines mark the locations of the SIGHT lines, and the grey dashed rectangle shows the surface location of subsequent figures. Plate motion (after DeMets *et al.* 1994) is displayed by a vector relative to a fixed Australian Plate. The 2000 m bathymetry contour indicates the continental margin.

anisotropy (Vauchez *et al.* 1998; Meissner *et al.* 2002). A 3-D approach is, therefore, required for the study of continental collisions, particularly in transpressional regimes where along-strike variations due to the asymmetry along the structural axis of the mountain belts can be expected.

New Zealand's South Island, where the Australian and Pacific continental plates collide obliquely (Fig. 1), is a relatively well-studied collision zone with excellent knowledge of the strain history. In the past 45 Ma there has been about 850 km of right lateral displacement through New Zealand, roughly half of which has been partitioned onto a single major fault, the Alpine fault (Sutherland 1999). During the last 6 or 11 Ma central South Island has experienced an additional lithospheric shortening of roughly 100 km (Walcott 1998; Cande & Stock 2004).

The crust in South Island accommodated this lithospheric shortening by the formation of the Southern Alps orogen and its crustal root (e.g. Wellman 1979; Woodward 1979; Koons 1990; Norris *et al.* 1990; Beaumont *et al.* 1996; Walcott 1998). Recent seismic images of lines 1 and 2 (Fig. 1) from the South Island GeopHysical Transect (SIGHT) experiment (Scherwath *et al.* 2003; Van Avendonk *et al.* 2004) show an increase in crustal thickness towards the south, about 7 km laterally within 50 km. This difference is largely in the thickness of the lower crust, suggesting flow of rheologically weak, highly ductile lower crust towards the south, a conclusion that has been suggested from geodynamic modelling (Gerbault *et al.* 2002).

The mantle can accommodate shortening by intracontinental subduction or simple lithospheric thickening (Molnar *et al.* 1999; Stern *et al.* 2000; Sutherland *et al.* 2000; Pysklywec *et al.* 2002). Mantle structures were modelled recently using teleseismic arrivals across central South Island (Stern *et al.* 2000; Molnar *et al.* 1999), and the data required a steep mantle anomaly of high seismic velocity directly beneath the deepest part of the root. The concept of simple lithospheric mantle thickening was given preference to subduction, because this process requires the least strain. Flexural studies (Stern *et al.* 2001) show that about 50 per cent of the loading on the lithosphere must be due to the mantle load, and that the flexural rigidity is low in the centre of South Island, conditions favouring lateral extrusion (Tapponnier *et al.* 1982). No extrusional creep in the mantle has been considered, however, as the observed strong seismic anisotropy can easily be explained by the strong mantle shear (Klosko *et al.* 1999; Molnar *et al.* 1999; Scherwath *et al.* 2002) without invoking lateral mantle creep.

Along the Southern Alps there occur lateral variations in gravity anomaly, plate convergence and seismic velocity structure. The gravity low in central South Island deviates from the strike of the plate boundary by 10–15 degrees, which is ascribed to the obliqueness of the collision (Reyners 1987; Gerbault *et al.* 2002). The amount of lithospheric shortening is larger in the north than in the south of South Island (Walcott 1998), whereas 3-D geodynamic modelling suggests that thickening and broadening of the crustal deformation is stronger in the south (Gerbault *et al.* 2002). Stern *et al.* (2000) created two 2-D structures of thickened lithospheric mantle from advances in teleseismic arrival times recorded along SIGHT lines 1 and 2 (Fig. 1). Kohler & Eberhart-Phillips (2002) derived a full 3-D model of upper mantle velocity anomalies from a tomographic inversion of teleseismic data from the Southern Alps Passive Seismic Experiment (SAPSE; see also Eberhart-Phillips & Bannister 2002). Both of these teleseismic studies found high-velocity anomalies in the mantle directly beneath the deepest part of the crustal root, but neither study could detect a significant difference in the anomaly from north to south. Some uncertainty, however, exists in these models as they both assume the upper mantle to be seismically isotropic, which is clearly not the case for this region (e.g. Klosko *et al.* 1999; Scherwath *et al.* 2002).

Gravity anomalies may be used to place constraints on mass anomaly distributions in the mantle; high-velocity anomalies, interpreted to be caused by colder mantle lithosphere submerged into hotter asthenosphere, produce a detectable positive density anomaly (Stern *et al.* 2000). The main aim of this paper is, therefore, to use gravity anomalies to investigate the 3-D structure of the oblique lithospheric compression in South Island. First, we compare topography and gravity and analyse isostacy in the region. This emphasizes the changes along the strike of the Southern Alps and indicates the need for 3-D investigations. Then we use gravity and the reasonably well-resolved crustal structures from SIGHT and SAPSE results (Godfrey *et al.* 2001; Scherwath *et al.* 2003; Van Avendonk *et al.* 2004; Eberhart-Phillips & Bannister 2002; Kohler & Eberhart-Phillips 2002) to place constraints on lithospheric mantle structures.

## 2 ISOSTATIC CONSIDERATIONS

In areas where local isostatic compensation occurs Bouguer gravity will show an inverse correlation with topography (Simpson *et al.* 1986; Watts 2001). The Southern Alps of New Zealand's South Island are no exception. The digital terrain model (DTM) and the Bouguer gravity field of South Island (Reilly *et al.* 1977) are shown in Fig. 2. High elevations have corresponding gravity lows. However, we note that the elevations are highest in a narrow band in central South Island (around $x/y = 225/25$ km), whereas the most negative gravity anomalies lie more to the south. The topography broadens slightly to the north and more so to the south, yet the gravity anomalies are significantly different in the north and the south.

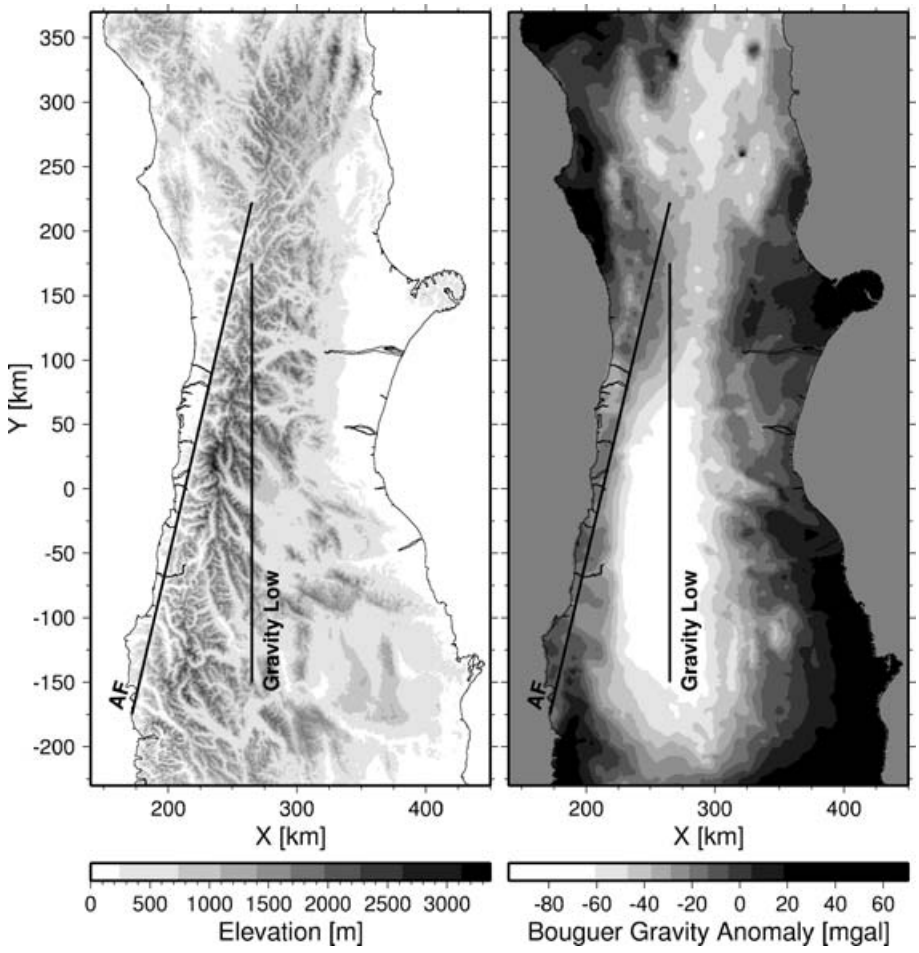


**Figure 2.** Comparison of topography and Bouguer gravity anomalies. The topography is from a digital terrain model resampled at 1 km from a higher resolution (25 m), and the Bouguer gravity field is from Reilly *et al.* (1977) with several more recent gravity surveys included. The error of the Bouguer field is up to 5 mGal in the mountains (Reilly 1972). The two straight lines show the orientations of the Alpine Fault (AF) and the South Island gravity low.

A comparison of smoothed topography with smoothed gravity anomalies exhibits better how the gravity field corresponds to the topography. This is because if Moho undulations are due to the loading of topography these undulations will produce long wavelength gravity anomalies, and the predicted gravity response is essentially inversely proportional to a smooth version of the topography. A smoothed Bouguer gravity field is free of short wavelength anomalies from shallow structures such as sedimentary basins or volcanic intrusions and would, therefore, compare better to topographic loading. We chose to smooth the data sets with a cosine filter of 100 km width because this coincides with the width of the gravity low in the southern half of the South Island, and furthermore represents roughly the minimum half width of the island. The elevation offshore was taken as zero.

Smoothed versions of topography and gravity are shown in Fig. 3. The smooth gravity field exhibits two lows; a small one in the north and a large one in the south. The smoothed elevations show a broad high in the north, an elongated but narrower high in the centre, and a broad area with shorter wavelength highs in the south. There are distinct differences in the comparison of gravity and topography as we go from north to south. Therefore, we have divided South Island into three zones for further analysis. Also noticeable in Fig. 3 is the deviation of the Alpine fault from the orientation of the gravity low by about 10–15 degrees, which has been ascribed to the oblique angle of the continental collision (Reyners 1987; Gerbault *et al.* 2002).

Profiles comparing elevations with gravity across each of the three zones are shown in Fig. 4. The bold lines represent the smoothed data sets, and in addition we show Bouguer, regional and isostatic gravity anomalies (Reilly *et al.* 1977). The regional gravity field used here is an interpolated field from Bouguer gravity measurements on basement rocks at least 2 km away from sediment basins. This so-called geological filter produced large data gaps around the extensive Tertiary basins at the east and west coasts of central South Island. These gaps were overcome by taking additional gravity readings offshore that were corrected by gravity modelling with constrained bathymetry (Ramillien & Wright 2000) and basin geometry and borehole measurements of sediment densities from Westland (Nathan *et al.* 1986) and Canterbury (Field *et al.* 1989). The profiles show that the smoothed elevations are higher but over a narrower zone in the centre (B) than to the north (A) and south (C), whereas the gravity becomes progressively more negative to the south. This trend is also clearly reflected in the isostatic gravity anomalies.

Isostatic gravity anomalies, which are the Bouguer gravity anomalies that have been corrected for the gravity effect of a predicted root, reveal how well the concept of compensating topographic loads at the Moho is established in a geographic region

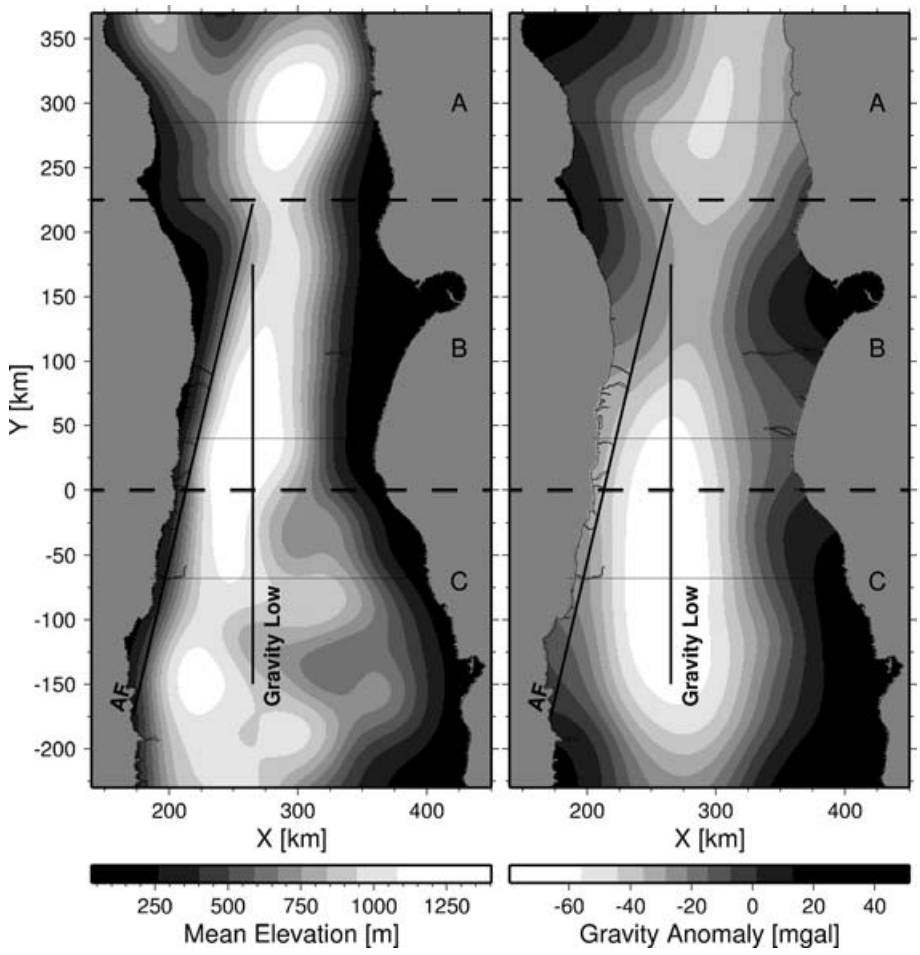


**Figure 3.** Comparison of mean elevations (left) and smooth gravity (right). The correlation of the two can be split into three zones: (A) Gravity field exhibiting shorter wavelength features than mean elevations in the north; (B) Good correlation between the two grids in the centre; (C) Gravity field exhibiting longer wavelength features than the mean elevations in the south. The thin lines represent characteristic profiles (Fig. 4) for isostatic considerations. The two thick straight lines show the orientations of the Alpine Fault (AF) and the South Island gravity low.

(e.g. Bott 1982). Positive isostatic gravity anomalies can occur where the Earth's strength resists bending and deformation when loaded by topography. This may well be the case for profile A (Fig. 4) as it is close to the west-dipping Hikurangi subduction, located to the north of Kaikoura Peninsula at $x/y = 350/300$, which may provide flexural support for the topographic loading, adding to the elastic strength of the lithosphere.

In comparison to profile A, profiles B and C (Fig. 4) show a different relationship between gravity and topography. Both these more southern profiles have more pronounced gravity lows associated with topographic highs, and the isostatic gravity is depressed accordingly. Profile C has a significant low of $-20$ to $-30$ mGal which indicates some form of 'overcompensation' of the mountain load, that is, that the root is deeper than expected for the surface load.

A relatively thick mountain root is documented by the crustal structure derived by the SIGHT experiment. Line 2 (Scherwath *et al.* 2003), between profiles B and C (along $y = 0$ in Fig. 3), has a 44-km-deep Moho beneath mountains of an average height of 1.2 to 1.4 km (dependent on the amount of smoothing). If we take the crustal thickness of ∼27 km at the coasts of South Island as a pre-loaded standard thickness, then the thickness of the root is ∼17 km. Assuming Airy isostacy the relationship of root thickness $r$ to mean elevation $h$, dependent on the densities of crust ($\rho_{\text{crust}}$) and mantle ($\rho_{\text{mantle}}$), is given by $r = h * \rho_{\text{crust}}/(\rho_{\text{mantle}} - \rho_{\text{crust}})$ (e.g. Bott 1982).

Taking typical values for the densities of crust and mantle, a locally compensated root would be around 6 to 8 km thick in this area. An expected root depth is, therefore, about 35 km. Thus, the Moho appears about 9 km too deep, and the root roughly twice as thick as mountain loading would suggest. This extra loading on the Moho probably stems from below, where lithospheric shortening has started the submergence of upper mantle into the hotter, less dense asthenosphere, where it forms a positive load (Stern 1995; Stern *et al.* 2000). A long wavelength positive gravity signal would be produced by this anomaly, and this could explain at least some positive isostatic gravity anomalies surrounding the isostatic gravity lows (Fig. 4).

What is not clear, however, is why the isostatic gravity low increases to the south while elevations decrease. One possibility is that the mantle anomaly is larger in the south. From geodynamic modelling, Gerbault *et al.* (2002) attributed the observation, that Bouguer gravity and elevation in this area do not correspond to each other, to lateral flow and increased thickening and broadening of a highly ductile lower crust towards the south. This hypothesis is matched by the crustal structures for the two transects crossing the land (Fig. 1),

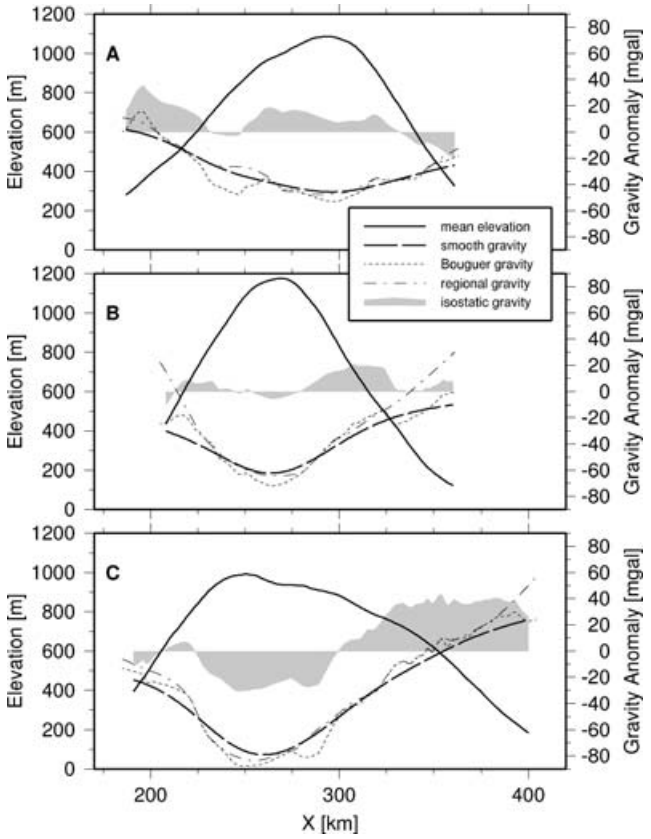


**Figure 4.** Topography and gravity from the three profiles of Fig. 3. Also shown are the Bouguer and isostatic gravity anomalies from Reilly *et al.* (1977) and regional gravity. See text for details.

where the Moho is 37 km deep in the north (Van Avendonk *et al.* 2004) and 44 km deep 50 km further to the south (Scherwath *et al.* 2003). This change is largely in a tripling of the thickness of the lower crust within the root zone in the south, whereas there is no change in lower crustal thickness under the northern transect.

Newest support for even larger crustal thicknesses further to the south comes from a recent crustal refraction experiment that ran from Fiordland in the south to north of Christchurch (Bourguignon *et al.* 2004). The estimated crustal thickness at Wanaka ($x/y = 275/-150$ on Fig. 3) is around 48 km, yet the topography is more subdued to the south (compare profiles B and C in Fig. 4). Bourguignon *et al.* (2004) also propose that the mantle lithosphere has thickened more in southern South Island than elsewhere and hence causes the thicker crust and a more negative isostatic gravity anomaly.

The qualitative analysis presented here is adequate to document the main features of the gravity field and its complex relationship to topography. However, it does not quantify the relative roles of isostatic compensation and the size and extent of the mantle anomaly in defining the relationship of gravity on topography. Analytical methods such as admittance and coherence functions could be used to establish the proper correlation between topography with gravity (e.g. Dorman & Lewis 1970). For a spectral analysis of the Bouguer gravity field the width of central South Island is small (<200 km), whereas wavelengths of deep subsurface loads (e.g. a mantle anomaly) can be in the order of 250–500 km (Ito & Taira 2000). Therefore, large areas offshore would need to be included. This is a daunting challenge because the proximity to the continent–ocean transition and two subduction zones would complicate the spectra as their wavelengths would overlap with the mantle anomaly.

## 3 GRAVITY ANALYSIS

Previous gravity analyses for the South Island region have provided a range of interpretations of its crustal structure. Reilly (1962) calculated a 7 km thickening of the crust using standard international empirical formulae relating topography to crustal thickness that were available at that time. Subsequent models, based on slightly different assumptions regarding gravity anomalies, have indicated crustal thicknesses ranging between 40 and 45 km (Woodward 1979, initial thickness 30 km plus 10–15 km of thickening) and 30–35 km (Allis 1986, initial thickness 25 km plus 5–10 km of thickening). Stern (1995) incorporated the whole lithosphere, including upper mantle density anomalies, into the gravity model and suggested a crustal thickening of 12–15 km below an initial thickness of 27 km.

Eberhart-Phillips & Bannister (2002) combined both gravity modelling and seismic tomography from local earthquakes and active source data from SIGHT to derive a 3-D velocity model for the South Island. Regional gravity was incorporated into the modelling below 20 km, assuming direct velocity-density relationships (Gardner *et al.* 1974; Hill 1978). These relationships, however, include velocity variations that are not associated with density anomalies, such as from high pore-fluid pressure or seismic anisotropy. High pore-fluid pressure is inferred to exist along the central South Island low-velocity zone (Stern *et al.* 2001), and seismic anisotropy has been directly measured in South Island schists (e.g. Okaya *et al.* 1995) and mantle (Klosko *et al.* 1999; Molnar *et al.* 1999), the latter at a depth as shallow as 25 km (Scherwath *et al.* 2002). Thus, a correlation of velocity and density has to be applied carefully in this region, ideally with seismic ray coverage equally distributed in all directions.

As noted above, crustal structures are now available from high resolution seismic data from the SIGHT experiment These new results provide the basis for a 3-D gravity analysis that follows. The aim of the modelling is to first employ 2-D gravity modelling to find those model parameters that would resolve a mantle anomaly as derived by the analysis of teleseismic data (Stern *et al.* 2000). Then, the same parameters are used in a 3-D model to constrain the shape of the mantle anomaly in 3-D.

### 3.1 2-D model

Structures found in the analysis of SIGHT line 2 (Scherwath *et al.* 2003) are used to define a 2-D gravity model. To detect the long wavelength gravity anomaly from the mantle density anomaly, or blob, only the deep structures are of interest here (Stern *et al.* 2000).

Fig. 5 shows the density model that produced the most realistic gravity anomaly, assumed to represent the expected mantle anomaly best. The density used for the mid-crust is 2750 kg m$^{-3}$, for the lower crust 3000 kg m$^{-3}$, and for the upper mantle 3300 kg m$^{-3}$. Note that outside the root zone the shallow mantle is considered to replace lower crust. The reference Moho for an undeformed crust was taken as 27 km (e.g. Scherwath *et al.* 2003). The 2-D gravity model extends infinitely beyond the model edges shown in Fig. 5, and 500 km both in and out of the model plane. An additional static shift of +5 mGal is applied to the predicted gravity anomaly based on a low-order global gravity field, arising from the difference between the Earth reference ellipsoid and the geoid (fig. 9.1a in Lambeck 1988), where the 5 mGal contour runs parallel along line 2.

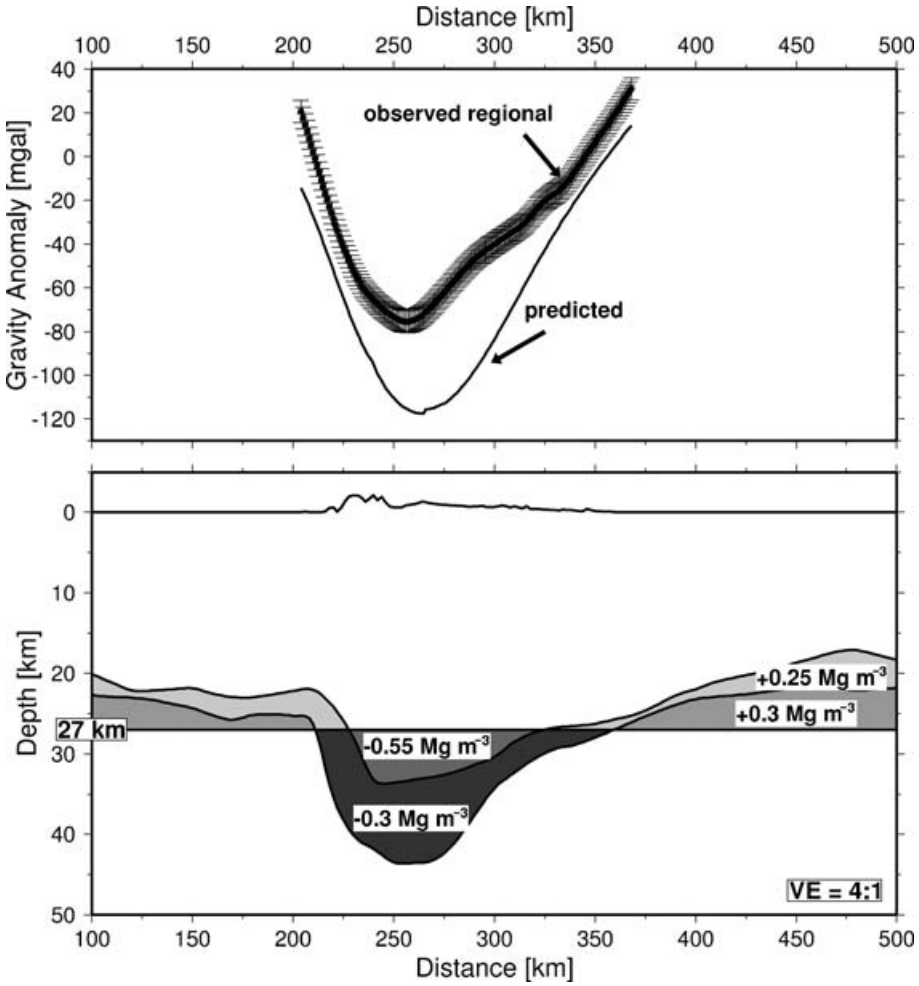


**Figure 5.** Gravity model of line 2, for deeper layers only, using density anomalies as shown in bottom panel. For absolute densities, refer to text. Vertical exaggeration of structure 4:1.

The difference between the predicted and the regional gravity anomaly (Fig. 6), hereinafter termed remnant field, is supposed to include the long wavelength gravity field of the mantle density anomaly that we are interested in plus a short wavelength residual from features in the crust that were not taken into account in this simple gravity model. To find the best-fitting structure for the mantle gravity anomaly, the model was extended to 250 km depth and divided into 10 km blocks. The mantle density anomaly was taken as $+40$ kg m$^{-3}$. Finally, the minimum depth to the density anomaly was set to 75 km, that is, 30 km below the deepest part of the root and 50 km below the Moho offshore, which is sufficiently deep for upper mantle to form an density anomaly in the asthenosphere (Stern *et al.* 2000). Using a simulated annealing inversion method, several solutions for the shape of the mantle anomaly were found, each similar to that shown in Fig. 6. The shape and location of the mantle blob is close to what was derived before (Molnar *et al.* 1999; Stern *et al.* 2000).

Some tests were run with different model parameters such as the densities of lower crust, mantle and asthenosphere, and also different reference levels for the Moho were used. The results were different sizes for the mantle anomaly, from considerably larger to relatively small. The parameters that are the most realistic and reproduced well the independently derived seismic velocity anomaly in the mantle were the final ones mentioned above and used for the following 3-D analysis.

### 3.2 3-D model

Extending the gravity modelling of the deep crustal structures to 3-D required interpolating the structural models from SIGHT line 1 (Van Avendonk *et al.* 2004), line 2 (Scherwath *et al.* 2003), line 3 (Godfrey *et al.* 2001), and line 3W (Melhuish *et al.* 2005). The velocity models of Eberhart-Phillips & Bannister (2002) and Kohler & Eberhart-Phillips (2002) were also incorporated, using the 7.0 and the 7.8 km s$^{-1}$ depth contours as indicators for the lower crust and Moho structures, respectively. Fig. 7 shows the final structures used. The gravity model was extended to the north and south where the analysis of Kohler & Eberhart-Phillips' (2002) derived a possible mantle anomaly distribution.

Although the regional gravity field from above extends over the entire South Island, only data from a limited area were used for the 3-D analysis here. The crustal structures are considered well defined around the main SIGHT lines (Fig. 7) but less so away from them. As the strongest influence on the gravity field comes from the closest structures, a cut-off distance of 50 km away from the main SIGHT lines was adopted to ensure minimize the effect of poorly

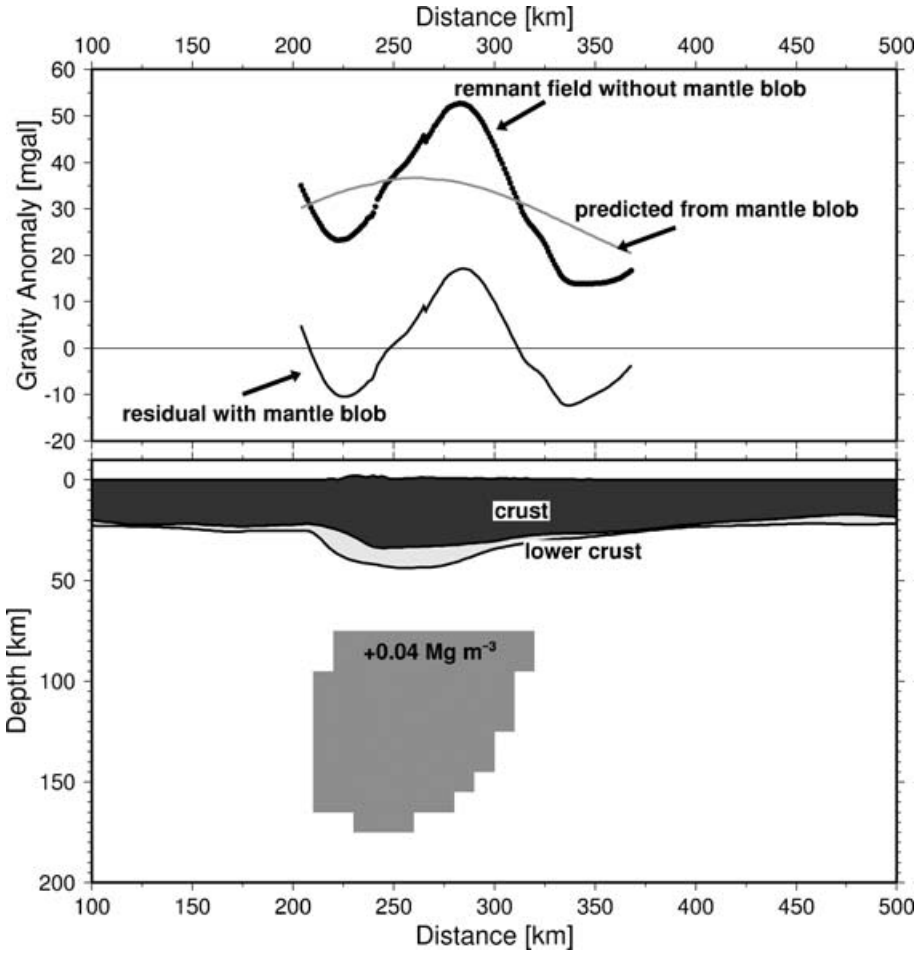


**Figure 6.** Inverted mantle anomaly on line 2, from minimizing the misfit of regional and predicted as shown in Fig. 5. Black dots are regional minus predicted from crust only, termed the remnant field. The grey line is the predicted gravity anomaly from the mantle anomaly. The black line is the final residual gravity anomaly, unexplained by either simple crustal structure or mantle blob. No vertical exaggeration. The mantle density anomaly is similar to Stern *et al.* (2000).

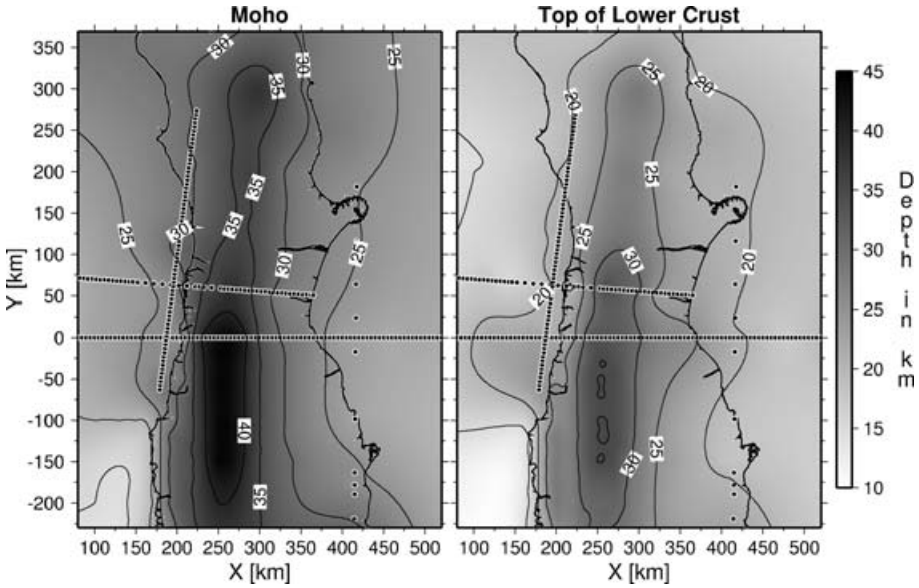


**Figure 7.** 3-D surfaces of top of lower crust and Moho, from SIGHT lines (black dots) and tomographic results (Eberhart-Phillips & Bannister 2002).

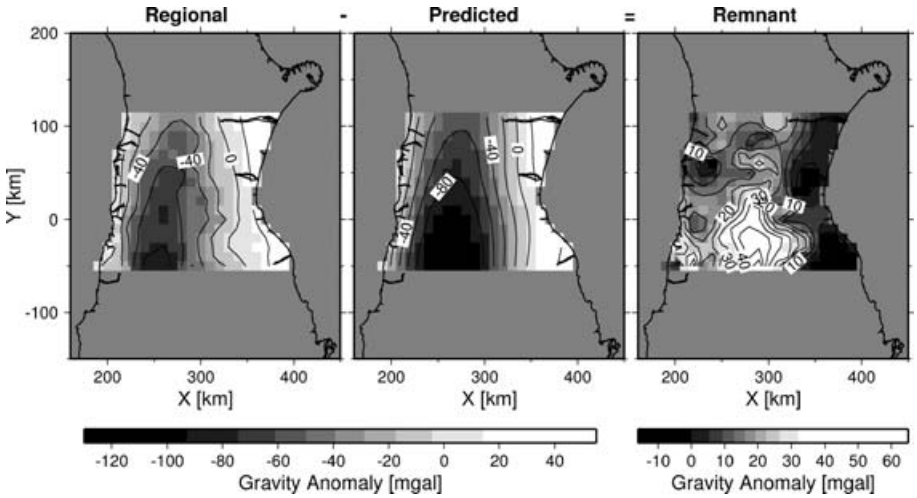


**Figure 8.** Gravity fields from 3-D modelling of the crustal structures. Density anomalies are defined as in Fig. 5, using 3-D surfaces of Fig. 7. Subtracting the predicted gravity anomaly (centre) from the regional (left) yields the remnant field (right).

defined structures on the gravity results. In addition, the distance to the two subduction zone systems north and south of South Island is at least 200 km, and the influence of the subducting slabs in the data is deemed negligible.

A similar modelling technique was used as for the 2-D analysis, with the same densities and reference Moho but with a more coarsely gridded model to keep the modelling computationally feasible. The final model block size for the mantle anomaly was 20 km cubed.

Fig. 8 shows the gravity fields used. The remnant field, which is the regional gravity minus the predicted gravity and thus similar to isostatic gravity, is mainly positive and it is interpreted as being caused by the shortened mantle. A stronger remnant field appears to the south of the SIGHT lines, implying that the mantle density anomaly is larger towards the south. The final inverted structures are given in Fig. 9.

The computed density anomaly in the mantle extends well beyond the location of the input gravity data. Therefore, the shape of the mantle density anomaly is only well constrained within the extent of the remnant gravity field, confined to central South Island, and discussed for that region. Furthermore, the ambiguity in this type of gravity analysis is large, as described above. A different depth of the reference Moho or different layer densities, would change the size of the mantle density anomaly, but only moderately its shape, that is, the mantle anomaly would always be larger in the south.

Gravity exhibits a clear trend through central South Island, as (a) the isostacy changes in character from north to south (Figs 3 and 4), and (b) 3-D gravity modelling gives evidence for a larger mantle mass anomaly towards the south (Fig. 9). However, Stern *et al.* (2000) found that the seismic velocity anomaly beneath SIGHT lines 1 and 2 does not need to vary in order to fit the observed teleseismic arrivals, that is, they could not detect a change within 50 km between the transects. This apparent contradiction may be explained by:

(1) velocity and density do not necessarily correlate (Barton 1986);

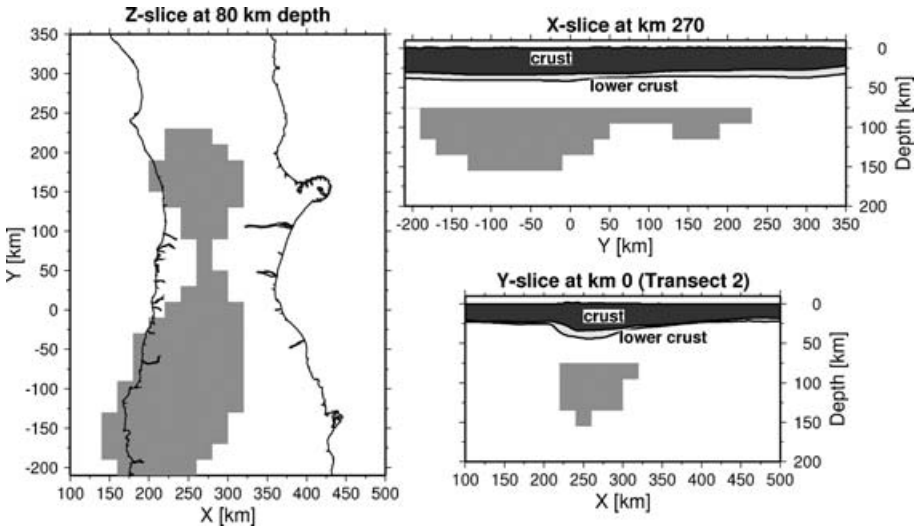


**Figure 9.** Inverted 3-D mantle density anomaly, from minimizing the misfit of regional and predicted as shown in Fig. 8, indicating maximum extent laterally (left) and in depth (top right). Also shown is depth slice along line 2 (bottom right) for comparison with Fig. 6. No vertical exaggeration.

(2) seismic anisotropy due to vertical (and not only horizontal) shearing in the mantle causes apparently higher velocities for the teleseismic signals further to the north and so less anomalous mantle material causes still similar seismic *P*-wave delays to the north and
(3) uncertainties in crustal thickness between lines 1 and 2.

What can be confirmed is the continuous high-velocity structure in the mantle as inferred by Kohler & Eberhart-Phillips (2002), an increased lithospheric thickening towards the south despite a decrease in lithospheric shortening (Walcott 1998; Cande & Stock 2004), and the total volume of the anomalous mantle material. The latter appears to be in the right order of magnitude considering the amount of crustal shortening, as suggested by the roughly 60 by 100 km area of the inverted 3-D mantle blob beneath line 2.

## 4 IMPLICATIONS

From Figs 3 and 4 it is clear that a north–south change in the parameters of isostatic compensation exists along South Island, and Fig. 9 shows that this can be resolved in terms of lithospheric mantle structures. In addition, the seismically imaged southward thickening of lower crust and crustal root (Scherwath *et al.* 2003; Van Avendonk *et al.* 2004) are the key factors that need to be considered to understand how lithospheric shortening is compensated at depth in this region. Together, these factors indicate that the lower lithosphere escaped to the south, that is, laterally almost perpendicular the axis of compression as common in young orogens (Meissner *et al.* 2002). The principal reason for this is the lowered viscosity of the lower crust (Gerbault *et al.* 2002) and upper mantle that cannot sustain the loading due to lithospheric thickening and, therefore, escapes by moving laterally.

Under the oblique compression in South Island, the orientation of the lower lithospheric thickening is predicted and observed to be about 10–15 degrees counter-clockwise from the plate boundary (Reyners 1987; Gerbault *et al.* 2002). This orientation, however, is not matched by the mantle density anomaly (Fig. 9). This difference may simply be due to the general ambiguity of gravity modelling, but it is also possible that the mantle anomaly partly reflects submerged 'missing' Eocene–Miocene oceanic lithosphere (Sutherland *et al.* 2000) which, predicted by plate reconstruction, has been overthrust by the plate boundary from the NE and has not yet been resolved. In this case, the mantle anomaly in Fig. 9 is likely to reflect both depressed upper mantle from continental collision and subducted oceanic plate from the south.

The separation of the anomalous cold mantle body into two parts, connected by a narrow neck under the highest part of the Southern Alps is only moderately well constrained. It reflects the reduction in the remnant mantle gravity anomaly, but we note the inherent simplification in the gravity modelling process. However, it does indicate that the highest mountains in South Island act as a prominent geographical marker for the shape of the entire lithosphere as immediately southwest of here a significantly larger lower lithospheric thickening is indicated.

Although plate motion data display more lithospheric shortening in the north than in the south (Walcott 1998; Cande & Stock 2004), more lower lithospheric thickening is predicted for the southern region. For these two results to be compatible, some form of lower lithospheric creep is necessary. In the deep crust this would be facilitated by the apparently highly ductile lower crust. For the lithospheric mantle, this creep would contribute to the extreme values of seismic anisotropy in this region (Klosko *et al.* 1999; Molnar *et al.* 1999), and would presumably produce more downwelling and sinking of the Moho in the south, which in turn would induce more lateral flow of lower lithosphere towards this sink. Lower lithospheric creep may also be a possible cause of the observed reflectivity in the lower crust (e.g. Kleffmann *et al.* 1998), but we consider that the decollement in the direction of compression (Little 2004) would be the major cause of the reflectivity (Jones & Nur 1984). Neither seismic anisotropy in the mantle nor reflectivity in the lower crust would, therefore, require the proposed lower lithospheric creep beneath the Southern Alps.

## 5 CONCLUSIONS

The comparison of topography and gravity in South Island, New Zealand, exhibits a trend that suggests a change in lithospheric loading from north to south. This can be related to changes in lithospheric structure, in particular Moho depth, lower crustal thickness and an anomalous mantle, manifest in a dense body of lithospheric mantle emplaced into the asthenosphere in this collisional regime. Recent crustal seismic data from central South Island show an increase in both Moho depth and lower crustal thickness southwards. Previous analyses of deeper, teleseismic data, however, did not detect a significant change in the size of a cold mantle body, or 'blob', along central South Island, yet gravity fields suggest some variation also in the upper mantle. We employ simple gravity modelling to obtain a mantle density anomaly and find that in three dimensions this dense mantle body is larger in the south than in the north. This finding is apparently in contrast to the amount of lithospheric shortening which is larger in the north, however it is consistent with results from geodynamic modelling and matches the trend in Moho depth and lower crustal thickness. We propose that the obliqueness of the compression with respect to the strike of the plate motion in New Zealand has introduced distributed lithospheric deformation perpendicular to the compression in central South Island, allowing lower lithospheric material to escape and creep south during its shortening.

## ACKNOWLEDGMENTS

We thank the editors and the two anonymous reviewers for their very constructive criticism. We also thank the Institute of Geological and Nuclear Sciences in New Zealand for making available their gravity database. MS is grateful to the University of Victoria, Canada, and NSERC for a post-doctoral fellowship during which part of the manuscript was written. All figures are produced by GMT (Wessel & Smith 1998).

## REFERENCES

Allis, R.G., 1986. Mode of crustal shortening adjacent to the Alpine Fault, New Zealand, *Tectonics,* **5**(1), 15–32.

Barton, P.J., 1986. The relationship between seismic velocity and density in continental crust—a useful constraint?, *Geophys. J. R. astr. Soc.,* **87,** 195–208.

Beaumont, C., Kamp, P.J.J., Hamilton, J. & Fullsack, P., 1996. The continental collision zone, South Island, New Zealand: comparison of geodynamical models and observations, *J. geophys. Res.,* **101**(B2), 3333–3359.

Bird, P., 1991, Lateral extrusion of lower crust from under high topography, in the isostatic limit, *J. geophys. Res.,* **96,** 10 275–10 286.

Bott, M.H.P., 1982, *The interior of the earth: its structure, constitution and evolution,* 2nd edn, Edward Arnold Publ. Ltd., London, UK.

Bourguignon, S., Savage, M., Stern, T. & Baldock, G., 2004. Mantle deformation and seismic anisotropy due to oblique collision, South Island, New Zealand, *EOS, Trans. Am. geophys. Un.,* **85**(47), Abstract T31A–1275.

Cande, S.C. & Stock, J.M., 2004. Pacific-Antarctic-Australian motion and the formation of the Macquarie Plate, *Geophys. J. Int.,* **157,** 399–414.

DeMets, C.G., Gordon, R.G., Argus, D.F. & Stein, S., 1994. Effect of recent revisions to the geomatgnetic time scale on estimates of current plate motions, *Geophys. Res. Lett.,* **21,** 211–214.

Dorman, L.M. & Lewis, B.T.R., 1970. Experimental isostacy, 1, Theory of the determination of the earth's isostatic response to a concentrated load. *J. geophys. Res.,* **75,** 3357–3365.

Eberhart-Phillips, D. & Bannister, S., 2002. Three-dimensional crustal structure in the Southern Alps region of New Zealand from inversion of local earthquake and active source data, *J. geophys. Res.,* **107**(B10), 2262, doi:10.1029/2001JB000567.

Field, B.D. *et al.*, 1989. *Cretaceous and Cenozoic sedimentary basins and geological evolution of the Canterbury Region, South Island, New Zealand,* New Zealand Geological Survey Basin Studies 2, New Zealand Geological Survey, Lower Hutt, New Zealand.

Gardner, G.H.F., Gardner, L.W. & Gregory, A.R., 1974. Formation velocity and density—the diagnostic basics for stratigraphic traps, *Geophysics,* **39,** 770–780.

Gerbault, M., Davey, F. & Henrys, S., 2002. Three-dimensional lateral crustal thickening in continental oblique collision: an example from the Southern Alps of New Zealand, *Geophys. J. Int.,* **150,** 770–779.

Godfrey, N.J., Davey, F., Stern, T.A. & Okaya, D., 2001. Crustal structure and thermal anomalies of the Dunedin Region, South Island, New Zealand, *J. geophys. Res.,* **106**(B12), 30 835–30 848.

Hill, D.P., 1978. Seismic evidence for the structure and Cenozoic tectonics of the Pacific Coast States, in *Cenozoic Tectonics and Regional Geophysics of the Western Cordillera,* Vol. 152, pp. 145–174, eds Smith, R.B. & Eaton, G.P., Geol. Soc. Am. Mem.

Houseman, G.A. & Molnar, P., 1997. Gravity (Rayleigh-Taylor) instability of a layer with non-linear viscosity and convective thinning of continental lithosphere, *Geophys. J. Int.,* **128,** 125–150.

Houseman, G.A., McKenzie, D.P. & Molnar, P., 1981. Convective instability of a thickened boundary layer and its relevance for the thermal evolution of continental convergence belts, *J. geophys. Res.,* **135,** 6115–6132.

Ito, G. & Taira, A., 2000. Compensation of the Ontong Plateau by surface and subsurface loading, *J. geophys. Res.,* **105,** 11 171–11 183.

Jones, T.D. & Nur, A., 1984. The nature of seismic reflections from deep crustal fault zones, *J. geophys. Res..,* **89,** 3153–3171.

Kleffmann, S., Davey, F., Melhuish, A., Okaya, D., Stern, T. & SIGHT Team, 1998. Crustal structure in the central South Island from the Lake Pukaki Seismic Experiment, *N. Z. J. Geol. Geophys.,* **41,** 39–49.

Klosko, E.R., Wu, F.T., Anderson, H.J., Eberhart-Phillips, D., McEvilly, T.V., Audoine, E. & Savage, M.K., 1999. Upper mantle anisotropy in the New Zealand region, *Geophys. Res. Lett.,* **26,** 1497–1500.

Kohler, M.D. & Eberhart-Phillips, D., 2002. Three-dimensional lithospheric structure below the New Zealand Southern Alps, *J. geophys. Res.,* **107**(B10), 2225, doi:10.1029/2001JB000182.

Koons, P.O., 1990. Two-sided orogen: collision and erosion from the sandbox to the Southern Alps, New Zealand, *Geology,* **18,** 679–682.

Lambeck, K., 1988. *Geophysical Geodesy: The Slow Deformation of the Earth,* Clarendon Press, Oxford, p. 718.

Little, T.A., 2004. Transpressive ductile flow and oblique ramping of lower crust in a two-sided orogen: insight from quartz grain-shape fabrics near the Alpine fault, New Zealand, *Tectonics,* **23,** TC2013, doi:10.1029/2002TC001456.

Meissner, R., Mooney, W.D. & Artemieva, I., 2002. Seismic anisotropy and mantle creep in young orogens, *Geophys. J. Int.,* **149**(1), 1–14.

Melhuish, A., Holbrook, W.S., Davey, F., Okaya, D.A. & Stern T., 2005, Crustal and upper mantle seismic structure of the Australian plate, South Island, New Zealand, *Tectonophys.,* **395**(1–2), 113–135.

Molnar, P. *et al.*, 1999. Continuous deformation versus faulting through the continental lithosphere of New Zealand, *Science,* **286,** 516–619.

Nathan, S., Anderson, H.J., Cook, R.A., Herzer, R.H., Hoskins, R.H., Raine, J.I. & Smale, D., 1986. *Cretaceous and Cenozoic sedimentary basins and geological evolution of the West Coast Region, South Island, New Zealand,* New Zealand Geological Survey Basin Studies 1, New Zealand Geological Survey, Wellington, New Zealand.

Norris, R.J., Koons, P.O. & Cooper, A.F., 1990. The obliquely convergent plate boundary in the South Island of New Zealand: implications for ancient collision zones, *J. Struct. Geol.,* **12,** 715–725.

Okaya, D., Christensen, N., Stanley, D. & Stern, T., 1995. Crustal anisotropy in the vicinity of the Alpine fault zone, *N. Z. J. Geol. Geophys.,* **38,** 579–583.

Pysklywec, R.N., Beaumont, C. & Fullsack, P., 2002. Lithospheric deformation during the early stages of continental collision: numerical experiments and comparison with South Island, New Zealand, *J. geophys. Res.,* **107**(B7), 2133, doi:10.1029/2001JB000252.

Ramillien, G. & Wright, I.C., 2000. Predicted seafloor topography of the New Zealand region: a nonlinear least squares inversion of satellite altimetry data, *J. geophys. Res.,* **105,** 16 577–16 590.

Reilly, W.I., 1962. Gravity and crustal thickness in New Zealand, *N. Z. J. Geol. Geophys.,* **5,** 228–233.

Reilly, W.I., 1972. The New Zealand gravity map series, *N. Z. J. Geol. Geophys.,* **15,** 3–15.

Reilly, W.I., Whiteford, C.M. & Doone, A., 1977. South Island: gravity map of New Zealand. 1:1000,000 Bouguer and isostatic anomalies, 1st edn, Department of Scientific and Industrial Research, Wellington, New Zealand.

Reyners, M., 1987. Subcrustal earthquakes in the central South Island, New Zealand, and the root of the Southern Alps, *Geology,* **15,** 1168–1171.

Scherwath, M., Melhuish, A., Stern, T. & Molnar, P., 2002. Pn anisotropy and distributed upper mantle deformation associated with a continental transform, *Geophys. Res. Lett.,* **29**(8), 1175, doi:10.1029/2001GL014179.

Scherwath, M., Stern, T., Davey, F.J., Okaya, D., Holbrook, W.S., Davies, R. & Kleffmann, S., 2003. Lithospheric structure across oblique continental collision in New Zealand from wide-angle P wave modeling, *J. geophys. Res.,* **108**(B12), 2566, doi:10.1029/2002JB002286.

Simpson, R.W., Jachens, R.C., Blakely, R.J. & Saltus, R.W., 1986. A new isostatic residual gravity map of the conterminous United States with a discussion on the significance of isostatic residual anomalies, *J. geophys. Res.,* **91,** 8348–8372.

Stern, T.A., 1995. Gravity anomalies and crustal loading at and adjacent to the Alpine Fault, New Zealand, *N. Z. J. Geol. Geophys.,* **38,** 593–600.

Stern, T.A., Molnar, P., Okaya, D. & Eberhart-Phillips, D., 2000. Teleseismic P-wave delays and modes of shortening the mantle lithosphere beneath South Island, New Zealand, *J. geophys. Res.,* **105,** 21 615–21 631.

Stern, T., Kleffmann, S., Okaya, D. & Scherwath, M., 2001. Low seismic wave-speeds and enhanced fluid pressure beneath the Southern Alps of New Zealand, *Geology,* **29,** 679–682.

Sutherland, R., 1999. Cenozoic bending of New Zealand basement terranes and Alpine fault displacement: a brief review, *N. Z. J. Geol. Geophys.,* **42,** 295–301.

Sutherland, R., Davey, F. & Beavan J., 2000. Plate boundary deformation in South Island, New Zealand, is related to inherited lithospheric structure, *Earth planet. Sci. Lett.,* **177,** 141–151.

Tapponnier, P., Peltzer, G., LeDain, A.-Y., Armijo, R. & Cobbold, P., 1982. Propagating extrusion tectonics in Asia: new insight from simple experiments with plastiline, *Geology,* **10,** 611–616.

Van Avendonk, H.J.A., Holbrook, W.S., Okaya, D., Austin, J.K., Davey, F. & Stern, T., 2004. Continental crust under compression: a seismic refraction study of South Island Geophysical Transect I, South Island, New Zealand, *J. geophys. Res.* **109**(B6), 6304, doi:10.1029/2003JB002790.

Vauchez, A. & Nicholas, A., 1991. Mountain building: strike-parallel displacements and mantle anisotropy, *Tectonophys.,* **185,** 183–201.

Vauchez, A., Tommasi, A. & Barruol, G., 1998. Rheological heterogeneity, mechanical anisotropy and deformation of the continental lithosphere, *Tectonophys.,* **296,** 61–86.

Walcott, R.I., 1998. Modes of oblique compression: Late Cenozoic tectonics of the South Island of New Zealand, *Rev. Geophys.,* **36,** 1–26.

Watts, A.B., 2001. Gravity anomalies, flexure and crustal structure at the Mozambique rifted margin, *Mar. Petrol. Geol.,* **18**(4), 445–455.

Wellman, H.W., 1979. An Uplift map for the South Island of New Zealand, and a model for uplift of the Southern Alps, in *The Origin of the Southern Alps,* Vol. 18, pp. 13–20, eds Walcott, R.I. & Cresswell, M.M., Royal Society of New Zealand Bulletin, New Zealand.

Wessel, P. & Smith, W.H.S., 1998. New version of generic mapping tools released, *EOS, Trans. Am. geophys. Un.,* **79,** 579.

Woodward, D.J., 1979. The crustal structure of the Southern Alps, New Zealand, as determined by gravity, in *The Origin of the Southern Alps,* Vol. 18, pp. 95–98, Walcott, R.I. & Cresswell, M.M., Royal Society of New Zealand Bulletin, New Zealand.